**RadioGraphics**

# New and Evolving Concepts in the Imaging and Management of Urolithiasis: Urologists' Perspective[1]

**LEARNING OBJECTIVES FOR TEST 1**

*After reading this article and taking the test, the reader will be able to:*

■ Discuss urologists' perspective on stone disease.

■ Describe the role of multidetector CT in diagnosis, treatment planning, and response assessment in patients with urolithiasis.

■ Identify radiation dose concerns and strategies for diminishing the associated risks.

**TEACHING POINTS**
*See last page*

*Avinash R. Kambadakone, MD, FRCR • Brian H. Eisner, MD • Onofrio Antonio Catalano, MD • Dushyant V. Sahani, MD*

Urolithiasis is a universal problem that has become increasingly prevalent in the United States and has a high rate of recurrence. Imaging of urolithiasis has evolved over the years due to technologic advances and a better understanding of the disease process. Computed tomography (CT) has been the investigation of choice for the evaluation of urinary stone disease. The emergence of multidetector CT and the recent introduction of dual-energy CT have further reinforced the superiority of this modality over other imaging techniques in the management of urolithiasis. Multidetector CT is not limited to simply helping make an accurate diagnosis in patients with stone disease; it is also useful in the assessment of stone burden, composition, and fragility, findings that are helpful in determining appropriate treatment strategies. In addition, multidetector CT is a valuable tool in the follow-up of patients after urologic intervention or institution of medical therapy. Familiarity with recent technologic developments will help radiologists meet the growing expectations of urologists in this setting. In addition, radiologists should be aware of the radiation risks inherent in the imaging of patients with urolithiasis and take appropriate measures to minimize this risk and optimize image quality.

©RSNA, 2010 • *radiographics.rsna.org*

---

**Abbreviations:** ASIR = adaptive statistical iterative reconstruction, KUB = kidney, ureter, bladder, PCNL = percutaneous nephrolithotomy, SSD = stone-to-skin distance, SWL = shock wave lithotripsy

©RSNA, 2010

## Introduction

Urolithiasis is a universal problem, affecting patients across geographical, cultural, and racial boundaries (1). The prevalence of urinary stones has progressively increased in the industrialized nations, and a similar trend is being observed in developing countries due to changing social and economic conditions (1–3). Approximately 1.2 million Americans are affected annually, and it is estimated that up to 14% of men and 6% of women will develop stone disease during their lifetime (4,5). In addition, many patients will be affected by multiple stones throughout their lifetime, with estimated recurrence rates of 50% within 5–10 years and 75% within 20 years. Recent studies have demonstrated an increasing overall prevalence, as well as an increase in the proportion of women with urinary stone disease over the last decade (6,7). The rising prevalence of urinary stone disease has had a significant impact on the healthcare system due to the direct costs involved and the morbidity associated with complications such as infection and chronic renal failure. The incremental cost of treatment for nephrolithiasis has been estimated to be approximately $3,500 per person in 2000 (8–10). In the United States, the annual healthcare burden of treating urolithiasis has risen from an estimated $1.83 billion in 1993 to $5.3 billion in 2000 (8–10).

Concomitant with the increasing prevalence of urolithiasis is the growing utilization of imaging for diagnosis, treatment planning, and posttreatment follow-up. Imaging in urolithiasis has evolved over the years due to technologic advances and a better understanding of the disease process. Since its introduction in the early 1990s, unenhanced computed tomography (CT) has become the gold standard for the evaluation of urinary stone disease at many centers—in both the emergency department and the clinic—replacing radiography and excretory urography (11–13). The emergence of multidetector CT in 1998 and the introduction of dual-energy CT techniques have further widened the scope of CT and reinforced its superiority over other imaging techniques in the management

of stone disease. Unenhanced CT performed in the emergency department for clinical suspicion of urolithiasis accounts for nearly 22% of all CT examinations performed for the evaluation of acute abdominal pain (14). Dalrymple et al (15) found that nearly 55% of patients undergoing CT for the evaluation of acute flank pain did not have stone disease, and about 15% had other abnormalities that were detected. Furthermore, the identification of ureterolithiasis at imaging has been found to alter management in nearly 55%–60% of patients suspected of having acute renal colic on the basis of clinical features and laboratory findings (15,16). The current role of multidetector CT extends beyond helping render an accurate diagnosis. Multidetector CT also provides information regarding stone burden, composition, and fragility, all of which is of immense therapeutic value, not only in the selection of treatment strategies, but also in predicting success.

In this article, we discuss urologists' expectations of imaging in the detection, quantification, and characterization of urinary stones. We also discuss the radiation risks associated with frequent multidetector CT examinations for urolithiasis and suggest various strategies for minimizing these risks.

## Stone Classification Based on Composition

A wide range of familial, environmental, dietary, and systemic factors contribute to the pathogenesis of renal stones (2). Stones are composed of a combination of crystals (both inorganic and organic) and proteins (Fig 1). Calcium-based stones, which include calcium oxalate monohydrate, calcium oxalate dihydrate, and calcium phosphate stones, account for 70%–80% of upper urinary tract stones. Struvite stones account for 5%–15% of stones and are composed of magnesium ammonium phosphate. In contrast, uric acid stones are unique in that they can often be dissolved with urinary alkalinization; they account for 5%–10% of stones and occur in acidic urine (pH <5.8). Other stones, including cystine, xanthine, and protein matrix stones, as well as drug (eg, triamterene, indinavir)–induced calculi, account for less than 5% of stones (1,17).
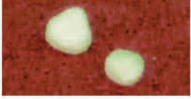
| Composition | Frequency of Occurrence | KUB Radiographic Appearance | CT Appearance/Attenuation (HU) | Associated Etiologic Factors |
|---|---|---|---|---|
| Calcium oxalate monohydrate and dihydrate (calcium oxalate dihydrate) | 40%–60% | Radiopaque | Opacified/ 1700–2800 | Underlying metabolic disorder (eg, idiopathic hypercalcuria or hyperoxaluria) |
| Hydroxyapatite (calcium phosphate) | 20%–60% | Radiopaque | Opacified/ 1200–1600 | Usually no metabolic abnormality |
| Brushite | 2%–4% | Radiopaque | Opacified/ 1700–2800 | . . . |
| Uric acid | 5%–10% | Radiolucent | Opacified/ 200–450 | Idiopathic hyperuricemia or hyperuricosuria |
| Struvite | 5%–15% | Radiopaque | Opacified/ 600–900 | Renal infection |
| Cystine | 1%–2.5% | Mildly opaque | Opacified/ 600–1100 | Renal tubular defect |

**Figure 1.**  Chart illustrates commonly occurring urinary tract stones and describes their salient features. *KUB* = kidney, ureter, bladder.

## Clinical Perspective

The most common symptom in patients with urolithiasis is acute flank pain, with dramatic relief upon passage of the stone (18). Stones that are impacted at the ureteropelvic junction produce flank pain, whereas stones lodged in the proximal ureter (between the ureteropelvic junction and the iliac vessels) cause flank pain radiating to the genitals (18). Stones lodged at the ureterovesical junction produce voiding urgency and suprapubic discomfort, and they cause pain that radiates into the groin and genitals (18,19). Associated symptoms include gross or microscopic hematuria, nausea, and vomiting. Struvite stones often remain asymptomatic without causing obstruction (18,20). Physical examination findings are usually nonspecific, and the examination should be targeted to rule out other abdominal conditions mimicking urolithiasis (11,15,18,21). A complete blood count and urinalysis are usually performed to rule out infection. Serum levels (eg, of electrolytes, blood urea nitrogen, creatinine, calcium, phosphorus, and uric acid) are determined to identify the cause of urolithiasis. Twenty-four-hour urine collections for detailed evaluation of metabolic abnormalities are usually reserved for patients with recurrent stones, children with stones, and identification of risk factors to guide management (18).

## Factors Influencing Treatment Decisions

The most important factors influencing decisions regarding urologic intervention are stone location, size, and composition, and patient symptoms (Figs 2, 3) (22). Renal stones (ie, stones located within the renal collecting system, above the ureteropelvic junction) may be treated with shock wave lithotripsy (SWL), ureteroscopy, or percutaneous nephrolithotomy (PCNL) (Table). The success of SWL, the least invasive of these three treatments, is related to a number of factors that may be evaluated with CT, including stone location (ie, lower pole of the kidney versus other calices), size, and composition, as well as stone-to-skin distance (SSD) (23–27). Ureteroscopy with lithotripsy, a transurethral endoscopic procedure that makes use of lasers, pneumatic lithotrites, or electrohydraulic lithotrites to fragment stones, is gaining popularity due to high stone-free rates and minimal morbidity (23,28–30). At many centers, ureteroscopy with lithotripsy is performed as an outpatient procedure with modern ureteroscopes as small as 7.4–9.0 F in diameter (29). This procedure is particularly useful in patients with stones that are refractory to SWL, as well as in patients with multiple stones, obesity, and bleeding diatheses. Although ureteroscopy with lithotripsy can be used for larger renal stones (ie, stones >2 cm), it is most commonly used to treat stones 0.5–1.5 cm in diameter (28). Finally, for larger stones, staghorn calculi, or lower pole stones that are refractory to SWL or ureteroscopy, PCNL is the treatment of choice (20). PCNL requires percutaneous ultrasonography (US) or fluoroscopically guided puncture of a renal calix, tract dilatation, and stone fragmentation-extraction (20,31). This procedure offers excellent stone-free rates for patients with large stones, and complications in modern series (most commonly, bleeding requiring transfusion or injury to adjacent organs) are low (0.8%–8% of cases) (20,31–33).

With regard to ureteral stones (ie, stones small enough to pass distal to the ureteropelvic junction and into the ureter), treatment often depends on stone size and type of interventional procedure (Figs 2, 3). The first-line treatment is medical expulsive therapy (α-blockers or calcium channel blockers with or without steroids and nonsteroidal anti-inflammatory medications), as well as hydration and analgesia (34).

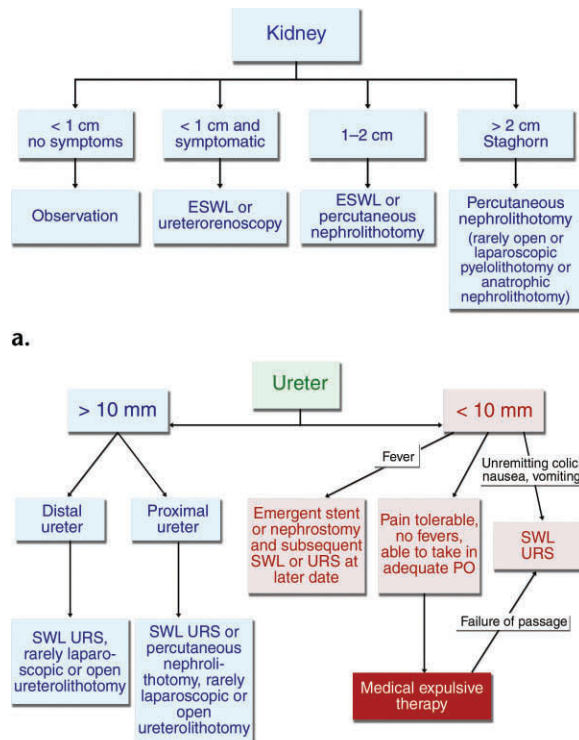A meta-analysis by Preminger et al (30) revealed that stones 5 mm or less in diameter



**Figure 2.** Flow charts depict treatment decisions based on stone location (kidney in **a**, ureter in **b**) and size. *ESWL* = extracorporeal shock wave lithotripsy, *PO* = per os (by mouth [ie, nutrition]), *URS* = ureteroscopy.

had a spontaneous passage rate of 68%, whereas stones greater than 5 mm but less than or equal to 10 mm had a spontaneous passage rate of 47%. Larger ureteral stones, or those that fail to pass with medical expulsive therapy, cause unremitting pain, nausea, or vomiting and may require intervention with SWL or ureteroscopy with fragmentation-extraction (30). PCNL is the first-line treatment for large ureteral stones (>15 mm), which are most commonly lodged in the upper ureter (30). Laparoscopic or open ureterolithotomy is rarely performed, but it may be used in certain refractory cases (35). As with renal stones, the outcome of ureteral stone treatment is affected by stone size, location, and composition.

## Imaging of Urolithiasis

### Conventional Imaging Techniques

Conventional abdominal (kidney, ureter, bladder [KUB]) radiography as the sole imaging modality for the evaluation of nephrolithiasis is limited by several factors, including bowel gas, extrarenal calcification, and large patient habitus. These factors diminish the sensitivity of KUB radiography
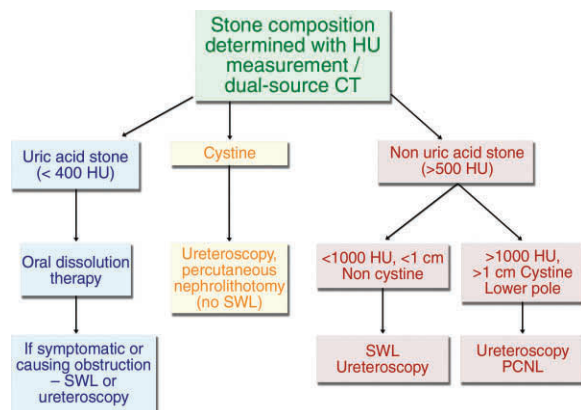
**Figure 3.**   Flow chart depicts treatment decisions based on stone composition. Cystine stones are typically resistant to SWL, with the degree of resistance being variable. *PCNL* = percutaneous nephrolithotomy.

**Salient Features of Various Urologic Interventional Procedures for Urolithiasis**

| Treatment | Clinical Indications | Advantages | Disadvantages |
|---|---|---|---|
| Common | | | |
| SWL | Stones <1 cm in kidney or proximal-distal ureter | Least invasive procedure, good success rate, may be performed with patient sedated (although anesthetic is sometimes used) | Poor success rates for high-attenuation stones (>1000 HU) and cystine stones |
| Ureteroscopy with lithotripsy (semirigid) | Stones <1 cm in distal ureter, proximal ureteral stones in women | High stone-free rate (slightly higher than with SWL), allows visualization and extraction of stones, is used to treat stones refractory to SWL | More invasive than SWL, requires general or spinal-epidural anesthesia |
| Ureteroscopy with lithotripsy (flexible) | Stones <1 cm in proximal ureter, stones <1.5 cm in kidney | High stone-free rate (slightly higher than with SWL), allows visualization and extraction of stones | More invasive than SWL, requires general or spinal-epidural anesthesia |
| PCNL | Stones >1.5 cm in kidney or proximal ureter, stones >1 cm in lower pole of kidney, staghorn calculi | Highest stone-free rates for large renal and upper ureteral stones and lower pole renal stones | More invasive than SWL and ureteroscopy, may require blood transfusion (<5% of cases) |
| Uncommon | | | |
| Open or laparoscopic ureterolithotomy | Large stones in middle or distal ureter | More effective than SWL or ureteroscopy for removing very large stones | Rarely used because other modalities are effective for treating the majority of stones and are less invasive |
| Open or laparoscopic pyelolithotomy | Large unbranched renal pelvic stones, large stones in a horseshoe kidney | More effective than SWL or ureteroscopy for removing very large stones, may be preferred modality for large stones in a horseshoe kidney if percutaneous access is difficult | Rarely used because PCNL has excellent success rates; in large renal stones with branches (ie, staghorn calculi), PCNL may have higher stone-free rates |
| Anatrophic nephrolithotomy | Full staghorn calculi (ie, branching into most or all of the minor calices) | Reasonable alternative to PCNL that requires more than two percutaneous tracts | Rarely used because most renal stones can be treated with PCNL via one or two tracts |

in the detection of urinary stones. However, KUB radiography is useful for planning fluoroscopically guided SWL and for monitoring the status of stone fragments after SWL, ureteroscopy, and PCNL (17). Intravenous urography fails to help detect urinary calculi in 31%–48% of cases and carries the risks associated with the injection of iodinated contrast material (17). Although widely available and cost effective, US has limited diagnostic value in the assessment of patients with suspected renal stones, even when performed by an experienced radiologist, particularly in the evaluation of distal ureteral calculi (17). Endovaginal and transperineal imaging have been found to be sensitive in the detection of small stones in the distal ureter; however, they are operator dependent and are not widely used (36).

## Computed Tomography

Unenhanced helical CT has gained widespread acceptance as the initial investigation of choice for the evaluation of patients with suspected urinary tract calculi (37,38). Since the first description of its utility by Smith et al (11) in 1995, unenhanced CT has been found to have a high degree of sensitivity (95%–98%) and specificity (96%–100%) in the diagnosis of urolithiasis (12,39–43). CT has several advantages over other imaging techniques: It can be performed rapidly, does not require the administration of contrast material, is highly sensitive for the detection of stones of all sizes, and allows the detection of other unsuspected extraurinary and urinary abnormalities (12,36,38). Extraurinary abnormalities including appendicitis, diverticulitis, pancreatitis, and gynecologic lesions such as ovarian torsion are often detected at CT in patients with nonspecific abdominal pain mimicking ureteral colic when the diagnosis may not be obvious prior to imaging (12,15,21,44). An additional benefit of CT is its ability to reveal urinary abnormalities such as congenital abnormalities, infections, and neoplasms, whose diagnoses have a greater clinical relevance than does that of stone disease (44).

## Multidetector CT

The introduction of multidetector CT in 1998 has opened up new prospects for CT in the imaging of urolithiasis. Advances in multidetector CT technology that allow the acquisition of isotropic volume data, and concurrent advances with respect to postprocessing algorithms and imaging workstations that allow multiplanar and three-dimensional evaluation of these isotropic data sets, have empowered radiologists to meet the greater

**Teaching Point**

---

STRUCTURED CT REPORT
TEMPLATE FOR UROLITHIASIS

DEMOGRAPHIC DETAILS:
Name:_____ Age:_____ Sex:_____
Date of Examination:_____
Indication for CT study:_____
Prior comparison CTs:_____
FINDINGS:
Stones present:   Y / N
Number of stones:_____

Location:    1. Side:  L / R
             2. Kidney: Upper pole / Mid pole / Lower
                pole / Renal pelvis / Staghorn
             3. Ureteropelvic junction
             4. Ureter:  Proximal (i.e. above sacroiliac
                vessels), distal (i.e. below sacroiliac
                vessels), ureterovesical junction
             5. Bladder

Size (mm):___   Volume (cc):___   Density (HU):___
Internal structure: Homogeneous / Heterogeneous
Stone to skin distance (cm):_____
Secondary signs:
        a) Hydronephrosis / Hydroureter
        b) Perinephric stranding
        c) Periureteral stranding
        d) Delayed renal excretion

Radiation dose:_____
Impression:_____

**Figure 4.**   Structured radiology report template for assessment of urolithiasis with multidetector CT.

expectations of urologists in the assessment of stone disease. Identification of the number, size, and location of calculi and determination of the presence of hydronephrosis (ie, obstruction) are routinely made with multidetector CT (Fig 4). High-resolution coronal reformatted images generated automatically from isotropic data sets obtained with 16–64-detector CT allow more rapid and accurate detection of urinary stones than do axial images alone (45,46). The quantification of stone burden with volumetric techniques, made feasible by the near-isotropic resolution of multidetector CT, holds great promise as both a tool for surgical planning and a predictor of treatment response (27,47,48). In addition, multidetector CT helps in the assessment of stone fragility and composition with use of attenuation measurements and characterization of internal structure (49–53). Differentiation between calcium-based stones and uric acid stones, previously achieved only with standard multidetector CT, has improved and is

a.

b.

**Figure 5.**   Ureteral stone in a 45-year-old man who presented with acute left flank pain. **(a)** Axial unenhanced multidetector CT scan shows a 4-mm stone in the left distal ureter (arrow). **(b)** Coronal reformatted image shows the left distal ureteral stone (arrow), along with a 2-mm stone in the left upper pole (arrowhead) that was not seen on the axial images. Secondary signs of ureterolithiasis, including perinephric stranding and thickening of the renal fascia, are also seen.

now also easily achieved with dual-energy CT, an exciting new CT innovation with capabilities of tissue differentiation (54).

***Multidetector CT Technique.***—The scanning technique and parameters for unenhanced multidetector CT for urolithiasis should be tailored to the indication. It is also important to keep in mind that a CT protocol for the evaluation of stone disease is not considered equivalent to routine unenhanced abdominopelvic CT. The former should typically include scanning of the entire urinary tract from the upper pole of the kidneys to the base of the urinary bladder (55). Although bladder distention has been recommended for enhanced visualization

of distal ureteral stones, the improved accuracy of multidetector CT due to the availability of coronal reformatted images usually obviates any patient preparation (45,46,55).

Thinner (1–3-mm) reconstruction sections are recommended for better detection and characterization of urinary calculi—particularly small stones, due to the reduction in partial volume averaging effect (13,56). However, acquiring 5-mm CT scans along with 3-mm coronal reformatted images has been found to improve stone detection while allowing radiation dose benefits (45,57,58). Acquiring CT scans with a section thickness greater than 5 mm or scanning at 10 mm can lead to frequent missing of small urinary calculi and can also affect size and attenuation measurements due to partial volume averaging effect resulting in lower average values (12,13). Therefore, images can be prospectively acquired at 5-mm collimation, and the near-isotropic data set obtained with scanners having 16 or more detector rows can then be reconstructed at a 1–3-mm section thickness to reduce errors in attenuation determination (13). In our practice, CT for stone evaluation is performed with a tube potential of 100–120 kVp and automatic tube current modulation with tube current ranging from 80 to 500 mAs (see "Radiation Dose").

Intravenous contrast material administration is not routinely required for the diagnosis of calculi at CT. In selected cases, however, contrast material administration may be useful for differentiating distal ureteral stones from phleboliths or vascular calcifications (59). In other scenarios, such as the incidental detection of tumor or other diseases on unenhanced scans, contrast material–enhanced CT may be required (11,59). Contrast-enhanced CT is also useful in conditions such as ureteral strictures, duplicated system, or uretero-pelvic junction obstruction, in which the delineation of aberrant genitourinary anatomy is necessary for effective treatment (59,60).

***Value of Coronal Reformatted Images.***—Axial imaging data sets are frequently used in the detection of renal stones. Coronal or sagittal reformatted images are used to supplement the axial scans in tracing the entire length of the ureter and in identifying the exact site of stone impaction, as well as in detecting small (1–2-mm) stones at the renal poles. Because the urothelial system is coronally oriented, the detection of urinary stones is not only quicker but also improved with coronal reformatted images (Fig 5) (45). In addition, the use of coronal reformatted images in conjunction

a.



b.
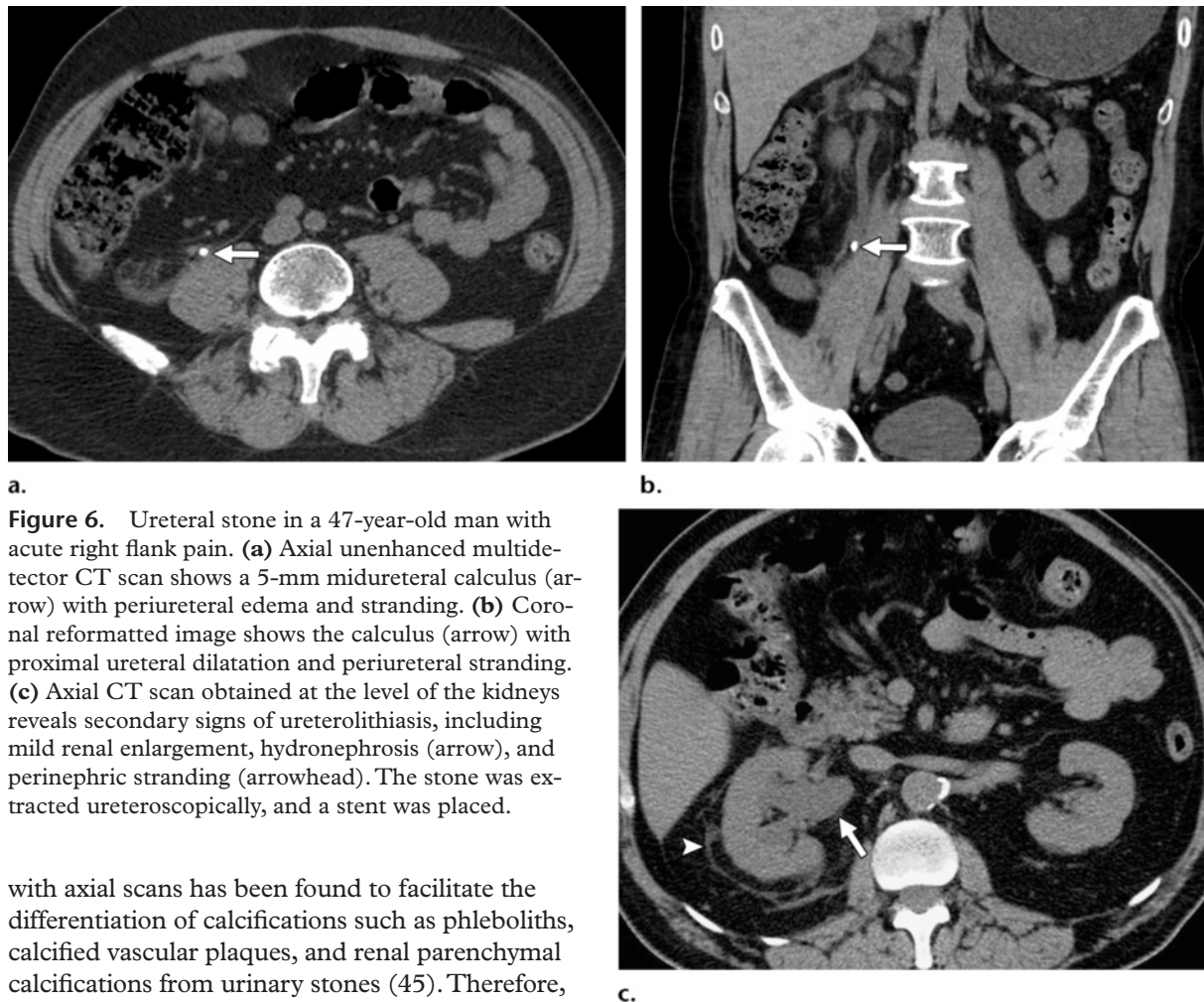
**Figure 6.**  Ureteral stone in a 47-year-old man with acute right flank pain. **(a)** Axial unenhanced multidetector CT scan shows a 5-mm midureteral calculus (arrow) with periureteral edema and stranding. **(b)** Coronal reformatted image shows the calculus (arrow) with proximal ureteral dilatation and periureteral stranding. **(c)** Axial CT scan obtained at the level of the kidneys reveals secondary signs of ureterolithiasis, including mild renal enlargement, hydronephrosis (arrow), and perinephric stranding (arrowhead). The stone was extracted ureteroscopically, and a stent was placed.



c.

with axial scans has been found to facilitate the differentiation of calcifications such as phleboliths, calcified vascular plaques, and renal parenchymal calcifications from urinary stones (45). Therefore, coronal reformation has been recommended as a useful adjunct to standard axial scanning, since it improves the detection of urinary stones that go unrecognized on axial scans and enhances radiologists' confidence (45,46).

***Multidetector CT Signs.***—Virtually all stones are visible at unenhanced CT, including those that are radiolucent on conventional radiographs, such as uric acid, xanthine, and cystine stones (21). These stones have an attenuation value (>200 HU) greater than that of the surrounding soft tissue, and multidetector CT helps accurately localize a stone within the renal pelvicaliceal system or ureter. The only stones that are difficult to visualize at CT are pure matrix stones and stones made of pure indinavir (a protease inhibitor used in the treatment of human immunodefi-

ciency virus infection) (21,61). These stones have soft-tissue attenuation (15–30 HU) and are likely to be missed at unenhanced CT (61,62). However, the distinctive clinical manifestation of renal colic in a patient receiving indinavir therapy for human immunodeficiency virus infection, along with the presence of obstructive features at CT, usually helps clinch the diagnosis (62). Intravenous contrast material may be administered in equivocal circumstances, with the stones being clearly depicted as filling defects in the contrast material–filled pelvicaliceal system or ureter on delayed phase images (62).

The most direct CT sign for ureterolithiasis is a stone within the ureteral lumen, with proximal ureteral dilatation and a normal distal caliber (Fig 6) (11,55). Ureteral dilatation may be absent in a small number of cases of ureterolithiasis.
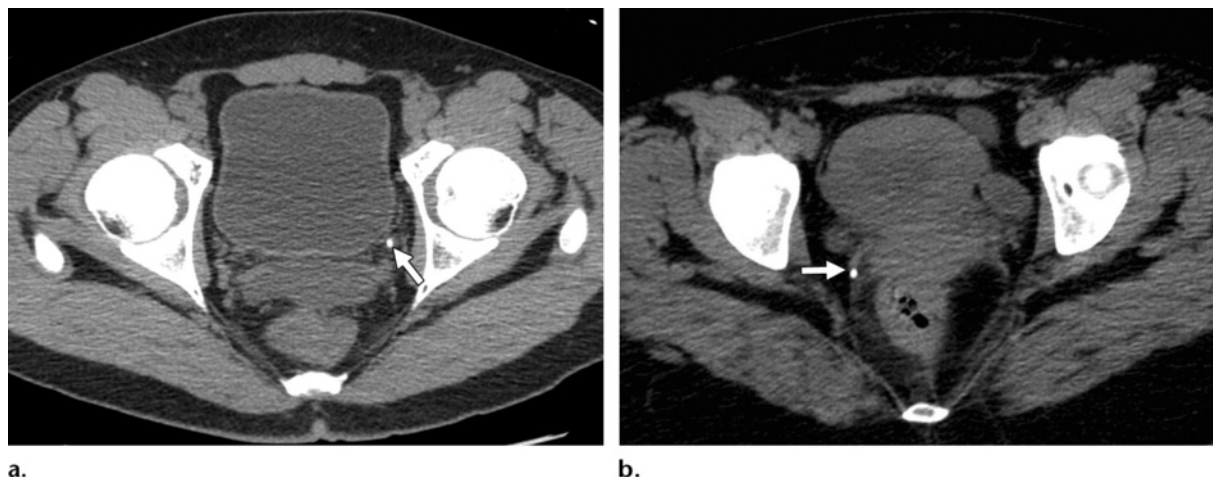
**Figure 7.** **(a)** Soft-tissue rim sign. Axial unenhanced multidetector CT scan obtained in a 44-year-old man with acute left pelvic pain shows a distal ureteral calculus (arrow) with surrounding soft-tissue attenuation that represents edema of the ureteral wall. **(b)** Comet tail sign. Axial unenhanced multidetector CT scan obtained in a 49-year-old woman shows the comet tail sign, created by an eccentric tapering soft-tissue area adjacent to a calcification (arrow).

Dalrymple et al (15) reported that in patients presenting with acute flank pain, ureteral stones are most likely to be lodged in the proximal (37% of cases) and distal (33%) portions, as opposed to the midureter (7%) and the ureterovesical junction (18%). The diagnosis of ureterolithiasis can be confirmed on the basis of several secondary signs at CT as well (21,37). The most reliable signs include hydroureter, hydronephrosis, perinephric stranding, periureteral edema, and unilateral renal enlargement (21,37). Perinephric fat stranding and dilatation of the intrarenal collecting system have a positive predictive value of 98% and a negative predictive value of 91% for the detection of ureteral calculi (37). Less reliable findings include unilateral absence of the white renal pyramid, thickening of the lateroconal fascia, and perinephric edema (21,37). Differences in renal parenchymal attenuation between obstructed and nonobstructed kidneys have also been used as a secondary sign of obstruction (21,37). Ege et al (37) reported that stones greater than 6 mm in diameter in the proximal ureter accompanied by more than five secondary signs of obstruction are more likely to necessitate intervention such as endoscopic removal or lithotripsy than are those with fewer secondary signs.

Extraurinary abdominal and pelvic calcifications such as phleboliths located in the expected course of the ureter on the symptomatic side may be mistaken for ureteral calculi. The routine use of coronal reformatted images, which allow tracking of the ureteral course, usually permits confident differentiation between calculi and other calcific processes. However, two signs, the "soft-tissue rim sign" and the "comet tail sign," have been described for the differentiation of ureteral stones from these calcifications (37,63). The soft-tissue rim sign consists of a halo of soft-tissue attenuation around a calcific focus and is very specific for ureteral calculi rather than phleboliths (37,63). The soft-tissue rim represents the edematous wall of the ureter around the calculus and has a sensitivity of 50%–77% and a specificity of 90%–100% (Fig 7a) (37,63). The presence or absence of the rim is found to correlate with the size of the calculus rather than the degree of obstruction (37,63). The comet tail sign is created by an eccentric, tapering soft-tissue area adjacent to the calcification and is a reliable feature in the diagnosis of phleboliths (Fig 7b) (37,63). Another feature that is helpful in differentiation is the central lucent area seen in phleboliths, in contrast to the opacified centers seen in calculi (37,63). After urologic intervention, residual stones often need to be distinguished from in situ stents or nephrostomy tubes for optimal planning of follow-up. In such situations, the use of bone window settings for image interpretation often helps in making a visual distinction between stent and stone (Fig 8) (64).
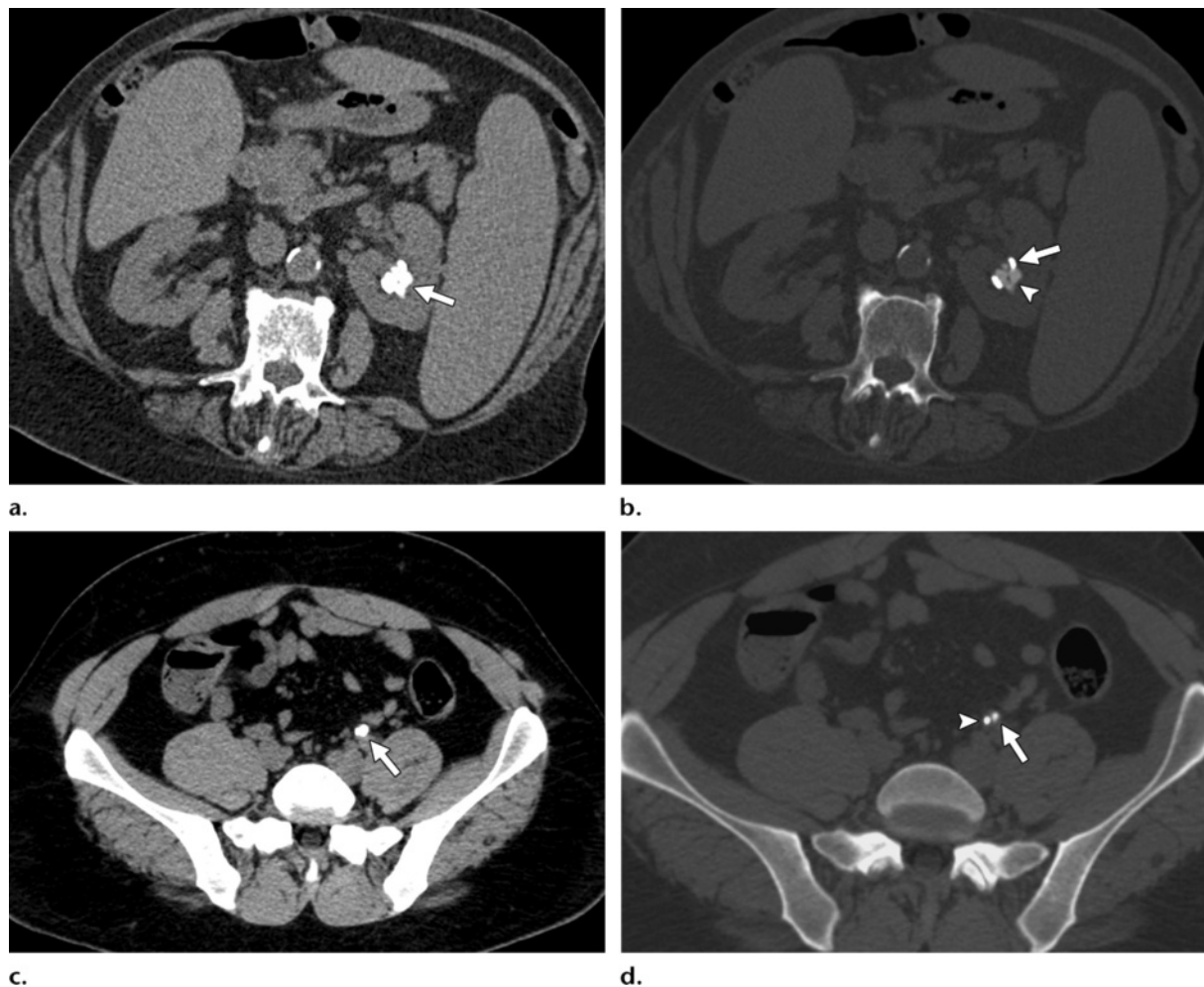
**Teaching Point**

**Figure 8.** Ureteral stents. **(a)** On an axial unenhanced multidetector CT scan (abdominal window settings [window width HU/window level HU = 400/30]), the proximal portion of a stent (arrow) is indistinguishable from renal pelvic stones. **(b)** On an axial CT scan (bone window settings [1120/300]), the stones (arrowhead) can be clearly distinguished from the stent (arrow). **(c)** Axial CT scan (abdominal window settings [400/30]) obtained in a different patient following ureteral stent placement shows a stent in the midureter (arrow). **(d)** CT scan (bone window settings [1120/300]) shows a 4-mm calculus (arrow) adjacent to but distinct from the stent (arrowhead).

Multidetector CT is often performed if urolithiasis is clinically suspected and may yield negative results. In such cases, it is quite unlikely that the stone was missed, and it is helpful to look at the involved side for secondary signs (21). If multidetector CT demonstrates unilateral ureteral dilatation and perinephric stranding, and a thorough search fails to reveal a stone, two possibilities are likely: Either the patient has recently passed the stone, or the stone is present but not of sufficient size or attenuation to be visible (21). On the other hand, if there is no ureteral dilatation or perinephric stranding, stone disease is highly unlikely. More often than not, acute flank pain mimicking

urolithiasis is secondary to other causes, such as appendicitis, endometrioma, hemorrhagic cyst, ovarian torsion, diverticulitis, pancreatitis, and so on (11,12). The section thickness of CT scans should also be considered, since stones less than 5 mm in diameter are often missed at scanning performed with a 10-mm section thickness.

***Stone Burden.***—Stone burden evaluation at CT is one of the most important factors in determining treatment strategies and management in cases of urolithiasis (20). The simplest and most common method of assessing stone burden is measurement of stone size. Measurement of stone size at CT is used to plan treatment and also helps accurately predict the rate of spontaneous
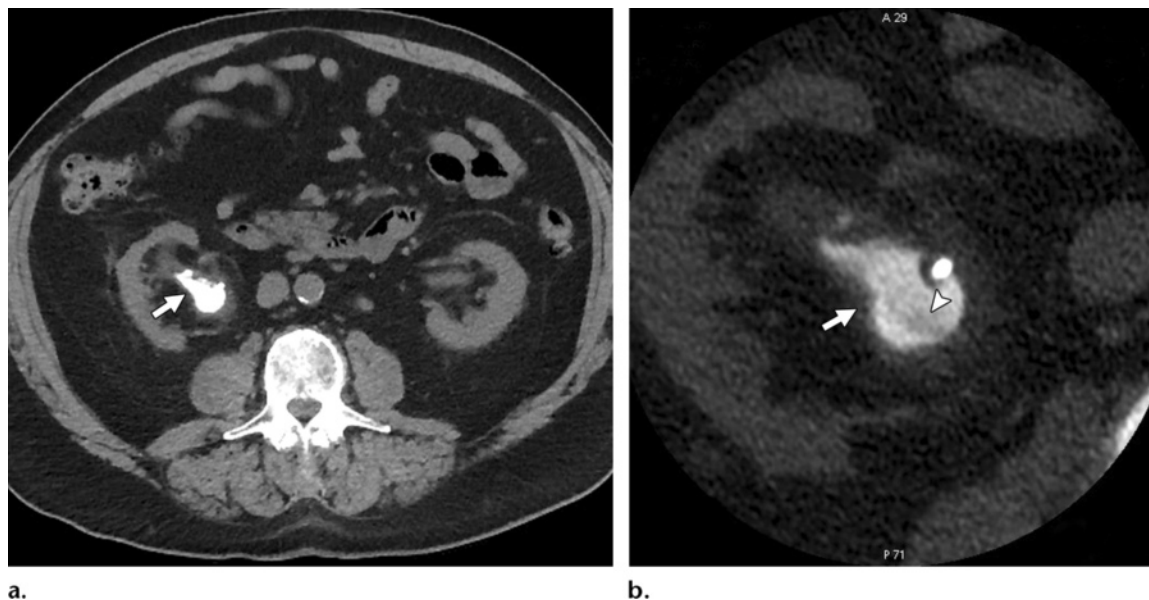
**Figure 9.** Staghorn calculus in a 63-year-old man. **(a)** Axial CT scan (abdominal window settings [400/30]) shows a staghorn calculus (arrow). **(b)** High-resolution CT scan (bone window settings [1120/300]) demonstrates internal inhomogeneities in the form of low-attenuation areas (arrowhead) within the calculus (arrow).

passage of ureteral stones, as discussed previously (30,65). Accurate measurement of stone size is of paramount importance because it helps determine whether a patient is a candidate for medical expulsive therapy or urologic intervention, as well as what type of intervention is most appropriate (ie, SWL, ureteroscopy with lithotripsy, or PCNL) (30). The greatest dimension of the stone is measured to the closest millimeter at CT. Although measurements have historically been performed with soft-tissue window settings (400/30), a recent study showed that the most accurate way to measure urinary stones is to use bone window settings (1120/300) with magnification (power of 4–5) (66).

Linear measurement methods commonly used at either spiral CT or conventional radiography pose a problem in the stone burden quantification of irregularly contoured stones such as staghorn calculi (27). Measuring the stone volume eliminates this problem because it takes into account the shape and diameter (in all dimensions) of the stone (27). Various authors have used different methods to calculate stone volume and hence to estimate stone burden, such as electronically tracing the stone circumference on all stone-bearing images to generate a three-dimensional volume measurement, or using the product of three orthogonal measurements (27,47,48). Novel semiautomatic segmentation tools can also be used to estimate stone volume. Stone volume

has been shown to be valuable for preoperative planning, and it is often useful to perform both linear and volumetric measurements of stone burden (27,47,48). In addition to being key to appropriate treatment planning, stone burden assessment can also be used to predict treatment success, particularly for procedures such as SWL (47,48). Wang et al (47) showed that a stone burden of more than 700 mm$^3$ as determined from the product of the three spatial dimensions is a significant predictor of failure for SWL.

***Stone Fragility.***—Knowledge of the internal structure of stones is another factor that can influence outcome following SWL, and it allows the clinician to be more selective in the choice of therapy. CT can be used to visualize the internal structure of stones, which is best appreciated when viewed with bone window settings and when imaged at high resolution with thin sections (67). At CT, the internal structure can be considered to be either heterogeneous or homogeneous. Heterogeneous stones are characterized by the presence of internal low-attenuation areas (voids or dark areas), whereas homogeneous stones have a uniform internal structure (Fig 9) (51). In vitro studies have shown that calcium oxalate monohydrate and cystine stones that appear heterogeneous at CT are more

fragile than those that appear homogeneous and require less comminution with SWL (68). It is believed that heterogeneity in stone composition renders a stone susceptible to fragmentation with treatment, since the irregularities in stone structure act as focal spots for shock wave energy and the stone disintegrates more easily (68). Conversely, homogeneous stones tend to be more rigid and therefore harder to break, often requiring more comminution and treatment sessions (51,68). Indeed, some authors suggest that the internal morphologic features of a stone rather than x-ray attenuation value correlates with the fragility of stones at SWL (51,68).

***Stone Composition.***—One of the key determinants of appropriate management in patients with urinary calculi is the knowledge of stone composition (Fig 3). Determination of stone composition is of particular importance because *(a)* uric acid stones may be treated with urinary alkalinization as a first-line treatment, with surgical treatment being reserved for stones that do not respond to medical therapy; and *(b)* stones of certain compositions (eg, cystine stones), as well as calcium-based stones of certain attenuation, are extremely difficult to fragment with SWL (51,69–71). Stone composition also affects the efficacy of extracorporeal SWL. Brushite, cystine, and calcium oxalate monohydrate stones are hard and more resistant to fragmentation with SWL (50,72–75). Historically, the clinical tools routinely used to infer stone composition have included urine pH, urinary crystals, prior stone history, presence of urea-splitting organisms, and conventional radiography (71,76). Ex vivo determination of stone composition is performed with infrared spectrophotometry or x-ray crystallography. More recently, there has been an increase in the use of CT for the assessment of stone composition (50,71,75). Determination of stone composition can be accomplished at CT on the basis of the attenuation values of stones and with the help of dual-energy scanning.

Bellin et al (50) reported that helical CT attenuation as well as stone density can be used to predict stone composition in vitro with 64%–81% accuracy. Uric acid, cystine, calcium oxalate monohydrate, and brushite calculi have been identified in vitro with an accuracy exceeding 85% on the basis of attenuation measurements (50,72–74). Although the attenuation

values of different types of stones (particularly struvite stones) vary among studies, CT is fairly accurate in helping predict stone composition in vitro (13,50,52,71,75). The attenuation values of urinary calculi at 120 kV usually fall within certain ranges: uric acid, 200–450 HU; struvite, 600–900 HU; cystine, 600–1100 HU; calcium phosphate, 1200–1600 HU; and calcium oxalate monohydrate and brushite, 1700–2800 HU (13,50,52,71,75).

Differentiation among stones is more complicated and less reliable in vivo. Among other factors, it is dependent on the size and accurate placement of the region of interest. Furthermore, attenuation measurement becomes more complicated in stones of mixed composition (35%–65% of stones) (1,77). Because stones of mixed composition, as well as struvite, cystine, and calcareous stones, have overlapping attenuation ranges in vivo, CT attenuation measurements have been most valuable in allowing differentiation of 100% uric acid stones from other stones (52). CT has not been shown to reliably help differentiate other types of stones or mixed stones (53). Moreover, CT attenuation measurements are affected by the section thickness, as reported by Ketelslegers and Van Beers (56), who found that stone attenuation decreased with an increase in section thickness.

Dual-energy CT performed with either a single or a dual x-ray tube represents a unique advance in CT that shows great promise in the determination of stone composition (78). This technique allows such assessment in a more robust manner, overcoming the limitations of measurements in Hounsfield units. A dual-source CT system is equipped with two x-ray tubes and two corresponding 64-detector arrays mounted on a gantry at a 90° angle (79). Dual-source CT allows concurrent scanning at two different energies (80 and 140 kVp), and the resulting data can be exploited for tissue material characterization (80). Differentiation of uric acid stones from other stones at dual-energy CT is facilitated by the inherent variation in the chemical composition of uric acid stones (composed of light elements such as hydrogen, carbon, nitrogen, and oxygen) compared with other types of stones such as calcium oxalate, calcium hydroxyapatite, cystine, and struvite stones, which are made up of heavy elements (eg, phosphorus, calcium, and sulfur) (80–82). This difference in chemical composition accounts for the variable x-ray attenuation properties of uric acid stones and other stone types at low and high
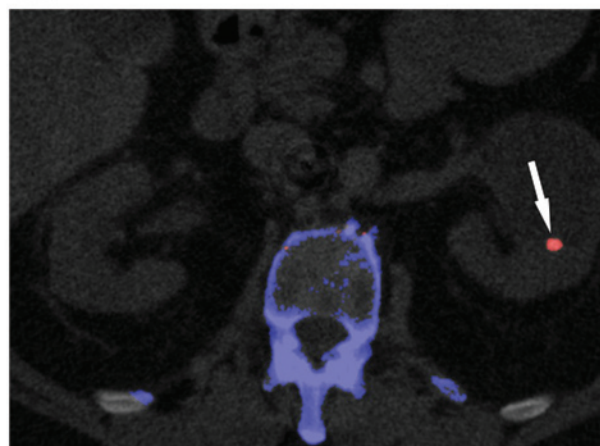
10a.
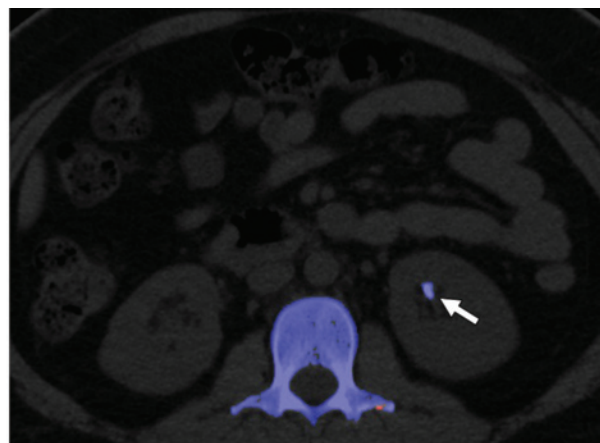
10b.
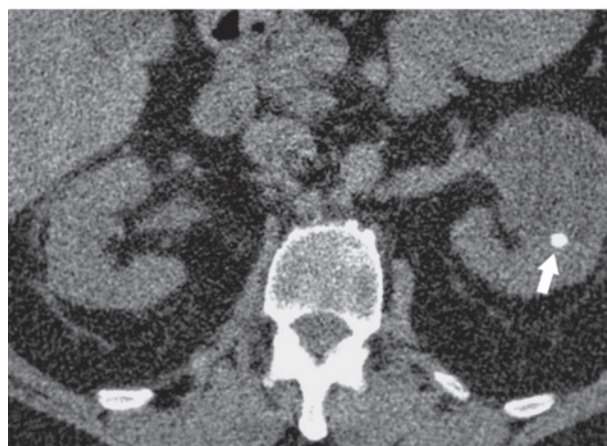
11a.

11b.

**Figures 10, 11.** **(10)** Calcium-based stone in a 36-year-old man who presented with acute left flank pain. **(a)** Initial axial unenhanced CT scan shows a calculus in the left midpole (arrow). Dual-energy CT (140/80 kVp) was performed in the region of the stone. **(b)** On a color-coded postprocessed image, the calculus is shown in blue (arrow), indicating a calcium-based stone. **(11)** Uric acid stone in a 46-year-old man who presented with acute left flank pain. **(a)** Initial axial unenhanced CT scan shows a calculus in the left midpole (arrow). Dual-energy CT (140/80 kVp) was performed in the region of the stone. **(b)** On a color-coded postprocessed image, the calculus is shown in red (arrow), indicating a uric acid stone.

kilovolt peaks (80–82). The dual-energy postprocessing software algorithm exploits this difference and assumes a mixture of water, calcium, and uric acid for every voxel of the scanned tissue (80–82). The voxels that have dual-energy behavior similar to that of calcium are color coded in blue, whereas those whose behavior is similar to that of uric acid are color coded in red (Figs 10, 11). The voxels that demonstrate linear attenuation behavior at the two different energies remain gray (80–82). With dual-energy CT, it is possible to differentiate between pure uric acid, mixed uric acid, and calcified stones (80–82). It is also possible to differentiate struvite stones from cystine stones by modifying the slope of three material decomposi-

tion algorithms (80–82). In a study involving a phantom model, Primak et al (82) demonstrated that dual-energy CT can help distinguish uric acid stones from other types of stones with 92%–100% accuracy depending on stone size and patient attenuation. Dual-energy scanning for renal stones involves initial standard unenhanced low-dose multidetector CT of the entire abdomen and pelvis using a single-source technique. Once a stone has been localized, targeted dual-energy scanning (140/80 kVp) of the anatomic region containing the stone is performed to substantially decrease the radiation exposure.

Dual-energy scanning can also be performed at single-source CT with rapid kilovolt peak switching, wherein an x-ray tube capable of rapid modulation of kilovoltage and milliamperage allows switching between low (80 kVp) and high (140 kVp) energy levels (78). Unlike dual-source CT, with its image-based dual-energy processing, this technique features dual-energy processing of projection data (78). In theory, this allows accurate material decomposition and monochromatic CT image display, which should potentially facilitate more precise tissue characterization and also substantially minimize imaging artifacts (78). Indeed, initial in vitro experiments have shown reliable results in the differentiation of uric acid, cystine, struvite, and calcium oxalate stones. Stolzmann et al (83) reported that dual-energy CT had a sensitivity and specificity of 89% and 98%, respectively, for the detection of stones containing uric acid.

***Treatment Planning.***—In addition to providing valuable information about stone characteristics such as size, orientation, and location, multidetector CT also aids in the presurgical planning of interventional procedures such as PCNL (84). One of the essential steps for successful percutaneous access is localization of the posterior calix (84). Although lower pole or posterior middle calix access is sufficient to attain a stone-free status for stones in the renal pelvis and inferior calix, access via the superior calix usually facilitates the removal of staghorn calculi, upper ureteral stones, and superior calciceal stones (84). Multidetector CT not only assists in the selection of an appropriate calix for percutaneous access, but it also helps ascertain a safe path for puncture by depicting the relationship of the kidney to various surrounding organs such as the spleen, liver, and colon (58). This is crucial, particularly in patients with spina bifida or severe scoliosis, in whom standard fluoroscopic guidance may be unsafe (58).

SSD as measured from the center of the stone to the skin surface on axial CT scans has been found to be a reliable predictor of stone-free status following SWL for lower pole renal stones (Fig 12) (26,70,85). Pareek et al (26) found that an SSD greater than 10 cm often resulted in failure to achieve stone-free status following SWL. Therefore, they suggested that ureteroscopic
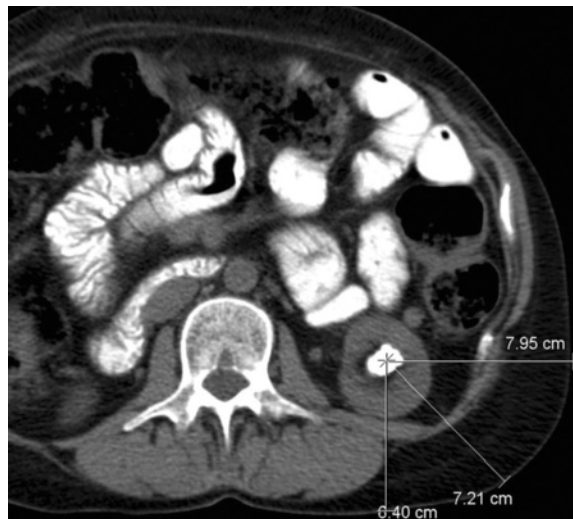


**Figure 12.** Measurement of SSD in a 65-year-old man with a left lower pole renal stone. On an axial unenhanced CT scan, the distance from the center of the stone to the surface of the skin at 0°, 45°, and 90° is 6.40, 7.21, and 7.95 cm, respectively. The mean of these three values is used to represent the SSD (7.2 cm in this case).

intervention or PCNL be performed in patients with an SSD greater than 10 cm at CT (26). Although Jacobs et al (86) did not find conclusive evidence of the reliability of SSD, other authors have highlighted its value at axial CT (26,70,85).

***Posttreatment Evaluation.***—Although it is critical to accurately determine stone characteristics prior to treatment to facilitate the selection of appropriate therapeutic strategies, it is also imperative to perform follow-up imaging after treatment. The purpose of imaging following either urologic intervention or medical therapy is essentially threefold: to confirm stone-free status, to identify the presence of residual stones, and to rule out obstruction in the urinary system (58). The additional advantage of CT following urologic intervention lies in the detection of complications such as perirenal hematoma and urinoma (87).

In the conservative management of ureteral stones, it is common practice to follow up patients with conventional radiography at 1–2-week intervals (21). Although multidetector CT is increasingly being used in the management of urolithiasis, repeat CT may not be the best follow-up option due to radiation concerns (21). The choice of imaging modality for the follow-up of these patients is usually made based on the visibility of the
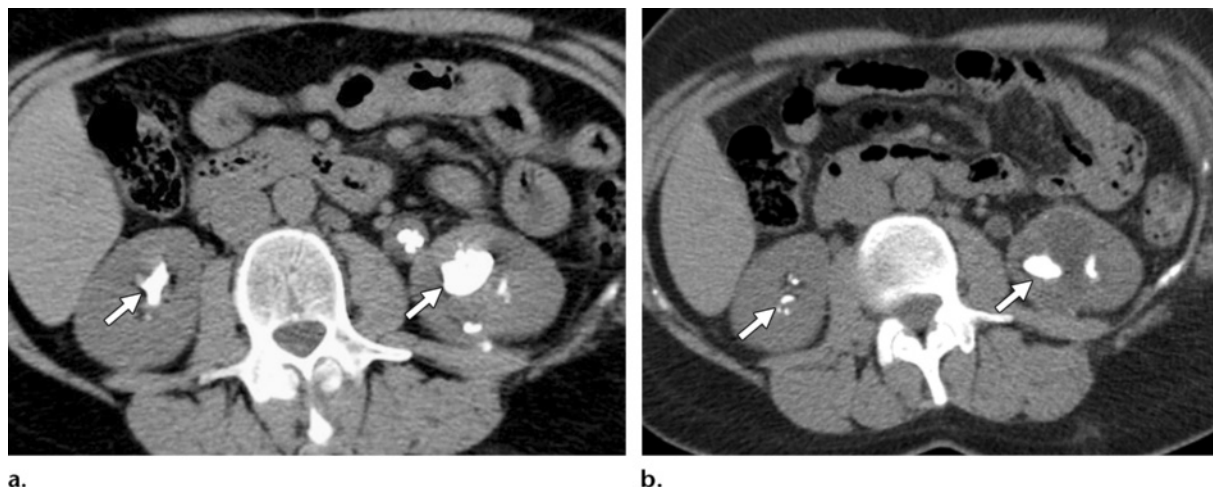
**Teaching Point**

a.  b.

**Figure 13.** Bilateral staghorn calculi in a 52-year-old man. **(a)** CT scan obtained prior to SWL shows bilateral staghorn calculi (arrows) with left proximal ureteral calculi. **(b)** Posttreatment CT scan shows several residual fragments in both renal pelves (arrows). The patient underwent PCNL for removal of the residual fragments.

stone on the CT scout images (21). If the stone is visible, conventional radiography is used for follow-up, with the CT scout images considered to be the baseline radiograph (21). The location and character of the stone on the scout images will help locate the stone on follow-up radiographs (21). If the stone is not visible on the scout images and is less than 5 mm in diameter, it is unlikely to be visible on a conventional radiograph and is likely to pass spontaneously (21). Stones greater than 10 mm that are not visible on the scout images probably represent uric acid or xanthine stones and usually will not be visible on conventional radiographs either (21). These patients need to be followed up with CT if management is conservative (21). However, because most of these patients undergo intervention, this is unlikely to be a cause of concern (21). Therefore, it seems reasonable to obtain conventional radiographs at the time of the CT study in patients with stones 5–9 mm in size (21). Reviewing conventional radiographs in conjunction with axial CT scans allows the expected location of the stone to be known precisely (21). It seems prudent to use a low-voltage technique to obtain CT scout images in patients with suspected ureterolithiasis, since this will increase stone conspicuity (21).

After urologic intervention, identification of residual stones is important because the recurrence rates are higher with persistent stone fragments (50%–80% of cases) than under stone-free conditions (10%–15%) (87). Recurrence is more

likely when residual fragments persist in the presence of urinary tract anomalies or in cases of infectious stones (87–91). CT is the preferred method for detecting residual stone fragments following PCNL and SWL, as well as for determining the need for a second-look procedure (Fig 13) (87,92,93). CT is particularly beneficial when complete stone clearance is desired or when the stones are faint or lucent at conventional radiography (94). However, Osman et al (94) reported that CT does not yield additional information when the residual stones are opaque on KUB radiographs or scout images. CT also helps identify the location of residual fragments in relation to the nephrostomy tract, thereby facilitating retrieval of the fragments and reducing stone burden (58,92,93). In addition, CT can alter the treatment approach on the basis of the detection of residual stones. For example, PCNL may be attempted following a failed SWL.

## Radiation Dose

Despite the immense benefits of multidetector CT, a key concern regarding its use in stone disease is the risk of radiation exposure (12,55,95). This is particularly true in young individuals who undergo repeated CT examinations due to recurrent stone disease and are consequently likely to be at risk for greater cumulative lifetime exposure (96–99). The reported effective radiation doses
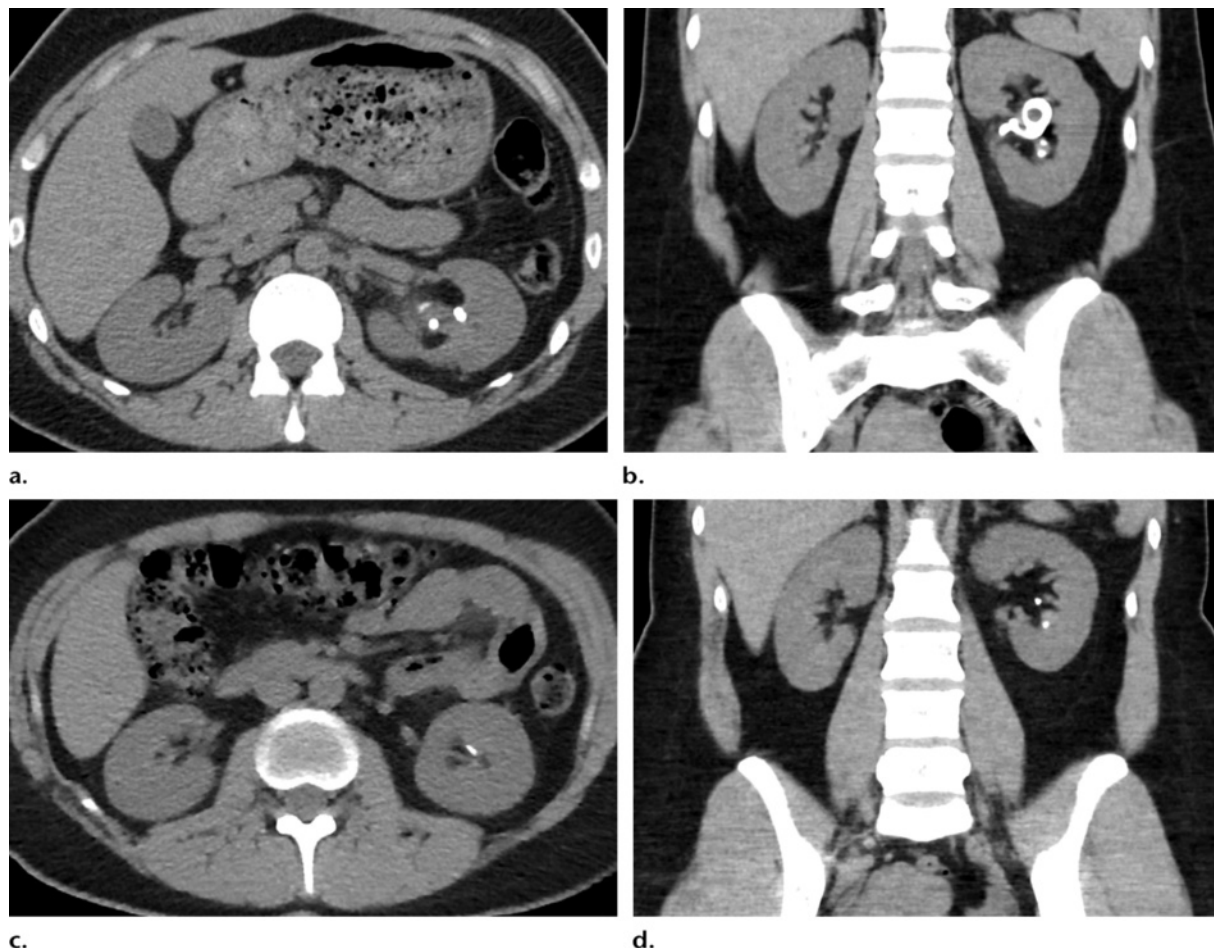
**Figure 14.** Radiation dose benefits of ASIR technique for a 43-year-old man with left renal calculi. **(a, b)** Axial **(a)** and coronal **(b)** CT scans obtained following stent placement show the left renal calculi. The radiation dose estimates for the CT examination were as follows: CT dose index volume, 10.4 mGy; dose-length product, 509.4 mGy/cm; and effective dose, 509.4 mGy/cm (ie, dose-length product) × 0.015 = 7.64 mSv. **(c, d)** Follow-up axial **(c)** and coronal **(d)** CT scans obtained 1 year later and reconstructed with ASIR technique (40% ASIR) show residual stones in the left renal pelvis. The radiation dose estimates for this follow-up examination were as follows: CT dose index volume, 5.6 mGy; dose-length product, 296.5 mGy/cm; and effective dose, 296.5 mGy/cm (ie, dose-length product) × 0.015 = 4.45 mSv. A dose reduction of 41.5% was achieved without any degradation of image quality.

with unenhanced CT range from 2.8 to 13.1 mSv for men and from 4.5 to 18 mSv for women, all of which are higher than with excretory urography (1.5 mSv for three-film and 2.1 mSv for six-film excretory urography) (98,100–102).

Numerous practical approaches for dose reduction in CT for urolithiasis have been advocated in the literature and practiced at our institution (96,103–106). Implementation of strategies targeted at dose reduction at every step of the CT protocol can considerably reduce the radiation dose for each CT examination. To begin with, limiting the scanning range is a useful step

that is particularly beneficial for follow-up studies. A default scanning range for urolithiasis routinely extends from the dome of the diaphragm down to the pelvic floor. Restricting the range to include only the kidney, ureter, and bladder (ie, scanning from the top of the kidneys to the base of the bladder) can reduce radiation dose by an amount equivalent to that used for 15–20 sections (107). In addition, performing focused studies with scanning limited to the areas of interest also minimizes radiation exposure (eg, scanning only the renal area to assess residual stone burden after urologic intervention). Use of 5-mm-thick sections for diagnostic acquisition supplemented by 2.5–3-mm coronal reformatted images is another
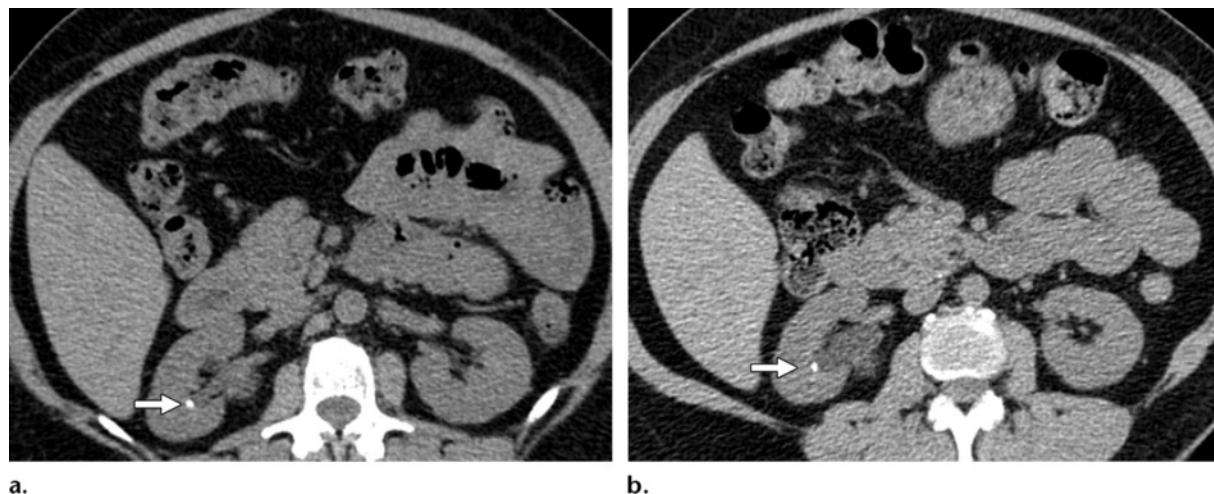
**Figure 15.** Benefits of reduced tube voltage for a 55-year-old man with a right midpole renal calculus. **(a)** Axial unenhanced CT scan (120 kVp, 240 mAs) shows the renal calculus (arrow). **(b)** Follow-up CT scan (100 kVp, 100 mAs) allows confident diagnosis of the renal calculus (arrow) in spite of increased noise in the image.

approach to reducing radiation dose without loss of diagnostic quality for stone detection. Studies have shown that use of 5-mm sections instead of the routine 1–3-mm sections can reduce the radiation dose by nearly 30%–50%.

The use of low-dose multidetector CT protocols in which the tube current (in milliamperes) and tube potential (kilovolt peak) are appropriately lowered has also been extensively studied in patients with calculus disease (106). Use of very low tube current (50–100 mAs) compared with that used for diagnostic examinations can offer radiation dose reduction of up to 80% while maintaining diagnostic performance for stone detection (96,103,104). An accuracy of 93%–97% has been achieved in the detection of urinary calculi with these low-dose techniques (95,96,98,101,103,104). However, use of a fixed tube current is not suitable for patients of different sizes; rather, scanning technique must be customized to the size of the patient (108).

Automatic tube current modulation technique is now available on all multidetector CT scanners and allows optimization of radiation dose in the x, y, and z planes on the basis of patient size and tissue density (105). Although automatic tube current modulation software differs among manufacturers in terms of techniques and nomenclature, all of the software relies on certain operator-defined parameters to accomplish the dual objectives of reducing radiation dose and improving diagnostic accuracy. Noise index and reference milliamperage are two such parameters that can be adjusted on multidetector CT scanners to opti-

mize radiation dose (105). Although a noise index of 10–15 is routinely used in abdominopelvic CT at our institution, elevating the noise index to 20–35 reduces the radiation dose by 40%–70%. In our experience, a noise index of 20 is preferred for initial CT performed for urolithiasis. Subsequent follow-up CT examinations are performed with increasing noise index levels (increments of 5 per examination up to 35). Despite the benefits of elevated noise index levels, it is important to realize that very high noise index levels can cause severe graininess of images and impact accuracy in the diagnosis of small calculi. One potential solution might be the use of certain image processing filters such as noise reduction filters, which are designed to eliminate excessive noise. Another solution is the use of new iterative image reconstruction algorithms, particularly the adaptive statistical iterative reconstruction (ASIR) technique, which eliminates image noise associated with low-dose CT (Fig 14). Analogous to the use of an elevated noise index, a low reference milliamperage of 100–160 mAs can serve as a practical means of achieving a lower radiation dose on multidetector CT scanners from other vendors (eg, Siemens).

Reducing the tube voltage not only has radiation dose benefits but also yields images with improved contrast, which is particularly advantageous for the detection of calculi (109). Lowering the tube voltage from 120 to 80 kVp reduces the dose per CT examination by 35%–57% (Fig 15) (109,110). On the other hand, lowering the tube

voltage without a proportionate increase in tube current results in degradation of image quality from noise and artifacts, which could potentially hamper the detection of small stones (109). A reasonable solution to this potential problem is the weight-based selection of tube voltage (80–140 kVp) (110). In general, patients weighing less than 150 lbs can be reliably imaged with 80–100 kVp, whereas for those between 150 and 300 lbs, a tube voltage of 120 kVp provides a good balance between radiation dose and image quality. In heavy patients (>301 lbs), a tube voltage of 140 kVp is recommended for radiation dose efficiency.

In spite of the continuing efforts to diminish radiation dose, caution is necessary to avoid "going overboard" with dose-reduction techniques. Low-dose CT can potentially degrade image quality in obese patients, and there remains a possibility of missing alternative diagnoses in selected patients with suspected urinary calculi (95,98). Therefore, customization of the scanning parameters to patient size and indication is necessary to facilitate achieving the dual objectives of improved image quality and diminished radiation exposure.

## Future Directions

Much of the emphasis of continuing research in multidetector CT for urolithiasis is directed toward optimization of radiation dose and characterization of stone composition. Among recent CT developments is the ASIR algorithm, which allows the elimination of image noise at low-dose CT, with a consequent reduction in radiation dose without affecting image quality or lesion conspicuity. Initial studies with this new technique have yielded promising results, with a dose reduction of nearly 20%–80%. On the diagnostic front, the development of computer-aided diagnostic methods for the detection of urinary stones is likely to have a major impact, facilitating rapid diagnosis and optimizing patient throughput. Computer-aided diagnostic algorithms for calculus detection can be designed on the basis of attenuation values and optimized to detect calcium-based stones.

## Conclusions

Multidetector CT currently plays an important management role in patients with urolithiasis, from the initial diagnosis in patients with acute flank pain to treatment planning and posttreatment follow-up. Keeping abreast of recent technologic developments will help radiologists meet the growing expectations of urologists. In addition, it is prudent to be aware of the radiation risk and to take appropriate measures to minimize this risk and optimize image quality.

## References

1. Moe OW. Kidney stones: pathophysiology and medical management. Lancet 2006;367(9507):333–344.
2. Curhan GC. Epidemiology of stone disease. Urol Clin North Am 2007;34(3):287–293.
3. Stamatelou KK, Francis ME, Jones CA, Nyberg LM, Curhan GC. Time trends in reported prevalence of kidney stones in the United States: 1976–1994. Kidney Int 2003;63(5):1817–1823.
4. Pak CY. Kidney stones. Lancet 1998;351(9118):1797–1801.
5. Soucie JM, Thun MJ, Coates RJ, McClellan W, Austin H. Demographic and geographic variability of kidney stones in the United States. Kidney Int 1994;46(3):893–899.
6. Pearle MS, Calhoun EA, Curhan GC. Urologic Diseases of America Project: urologic diseases in America project—urolithiasis. J Urol 2005;173(3):848–857.
7. Scales CD Jr, Curtis LH, Norris RD, et al. Changing gender prevalence of stone disease. J Urol 2007;177(3):979–982.
8. Clark JY, Thompson IM, Optenberg SA. Economic impact of urolithiasis in the United States. J Urol 1995;154(6):2020–2024.
9. Saigal CS, Joyce G, Timilsina AR. Urologic Diseases in America Project: direct and indirect costs of nephrolithiasis in an employed population—opportunity for disease management? Kidney Int 2005;68(4):1808–1814.
10. Trinchieri A. Epidemiological trends in urolithiasis: impact on our health care systems. Urol Res 2006;34(2):151–156.
11. Smith RC, Rosenfield AT, Choe KA, et al. Acute flank pain: comparison of non-contrast-enhanced CT and intravenous urography. Radiology 1995;194(3):789–794.
12. Smith RC, Verga M, McCarthy S, Rosenfield AT. Diagnosis of acute flank pain: value of unenhanced helical CT. AJR Am J Roentgenol 1996;166(1):97–101.
13. Saw KC, McAteer JA, Monga AG, Chua GT, Lingeman JE, Williams JC Jr. Helical CT of urinary calculi: effect of stone composition, stone size, and scan collimation. AJR Am J Roentgenol 2000;175(2):329–332.
14. Rosen MP, Siewert B, Sands DZ, Bromberg R, Edlow J, Raptopoulos V. Value of abdominal CT in the emergency department for patients with abdominal pain. Eur Radiol 2003;13(2):418–424.
15. Dalrymple NC, Verga M, Anderson KR, et al. The value of unenhanced helical computerized tomography in the management of acute flank pain. J Urol 1998;159(3):735–740.
16. Wrenn K. Emergency intravenous pyelography in the setting of possible renal colic: is it indicated? Ann Emerg Med 1995;26(3):304–307.
17. Sandhu C, Anson KM, Patel U. Urinary tract stones. I. Role of radiological imaging in diagnosis and treatment planning. Clin Radiol 2003;58(6):415–421.

18. Goldfarb DS. In the clinic: nephrolithiasis. Ann Intern Med 2009;151(3):ITC2.

19. Eisner BH, Reese A, Sheth S, Stoller ML. Ureteral stone location at emergency room presentation with colic. J Urol 2009;182(1):165–168.

20. Preminger GM, Assimos DG, Lingeman JE, Nakada SY, Pearle MS, Wolf JS Jr. AUA Nephrolithiasis Guideline Panel. Chapter 1. AUA guideline on management of staghorn calculi: diagnosis and treatment recommendations. J Urol 2005;173(6):1991–2000.

21. Smith RC, Coll DM. Helical computed tomography in the diagnosis of ureteric colic. BJU Int 2000;86(suppl 1):33–41.

22. Preminger GM, Vieweg J, Leder RA, Nelson RC. Urolithiasis: detection and management with unenhanced spiral CT—a urologic perspective. Radiology 1998;207(2):308–309.

23. Pearle MS, Lingeman JE, Leveillee R, et al. Prospective, randomized trial comparing shock wave lithotripsy and ureteroscopy for lower pole caliceal calculi 1 cm or less. J Urol 2005;173(6):2005–2009.

24. Perks AE, Gotto G, Teichman JM. Shock wave lithotripsy correlates with stone density on preoperative computerized tomography. J Urol 2007;178(3 pt 1): 912–915.

25. Weld KJ, Montiglio C, Morris MS, Bush AC, Cespedes RD. Shock wave lithotripsy success for renal stones based on patient and stone computed tomography characteristics. Urology 2007;70(6):1043–1046; discussion 1046–1047.

26. Pareek G, Hedican SP, Lee FT Jr, Nakada SY. Shock wave lithotripsy success determined by skin-to-stone distance on computed tomography. Urology 2005;66(5):941–944.

27. Bandi G, Meiners RJ, Pickhardt PJ, Nakada SY. Stone measurement by volumetric three-dimensional computed tomography for predicting the outcome after extracorporeal shock wave lithotripsy. BJU Int 2009;103(4):524–528.

28. Breda A, Ogunyemi O, Leppert JT, Lam JS, Schulam PG. Flexible ureteroscopy and laser lithotripsy for single intrarenal stones 2 cm or greater: is this the new frontier? J Urol 2008;179(3):981–984.

29. Hudson RG, Conlin MJ, Bagley DH. Ureteric access with flexible ureteroscopes: effect of the size of the ureteroscope. BJU Int 2005;95(7):1043–1044.

30. Preminger GM, Tiselius HG, Assimos DG, et al. 2007 guideline for the management of ureteral calculi. Eur Urol 2007;52(6):1610–1631.

31. Lee KL, Stoller ML. Minimizing and managing bleeding after percutaneous nephrolithotomy. Curr Opin Urol 2007;17(2):120–124.

32. Chibber PJ. Percutaneous nephrolithotomy for 1–2 cm lower-pole renal calculi. Indian J Urol 2008;24 (4):538–543.

33. Soucy F, Ko R, Duvdevani M, Nott L, Denstedt JD, Razvi H. Percutaneous nephrolithotomy for staghorn calculi: a single center's experience over 15 years. J Endourol 2009;23(10):1669–1673.

34. Hollingsworth JM, Rogers MA, Kaufman SR, et al. Medical therapy to facilitate urinary stone passage: a meta-analysis. Lancet 2006;368(9542):1171–1179.

35. Wolf JS Jr. Treatment selection and outcomes: ureteral calculi. Urol Clin North Am 2007;34(3): 421–430.

36. Mitterberger M, Pinggera GM, Maier E, et al. Value of 3-dimensional transrectal/transvaginal sonography in diagnosis of distal ureteral calculi. J Ultrasound Med 2007;26(1):19–27.

37. Ege G, Akman H, Kuzucu K, Yildiz S. Acute ureterolithiasis: incidence of secondary signs on unenhanced helical CT and influence on patient management. Clin Radiol 2003;58(12):990–994.

38. Heneghan JP, McGuire KA, Leder RA, DeLong DM, Yoshizumi T, Nelson RC. Helical CT for nephrolithiasis and ureterolithiasis: comparison of conventional and reduced radiation-dose techniques. Radiology 2003;229(2):575–580.

39. Boulay I, Holtz P, Foley WD, White B, Begun FP. Ureteral calculi: diagnostic efficacy of helical CT and implications for treatment of patients. AJR Am J Roentgenol 1999;172(6):1485–1490.

40. Fielding JR, Silverman SG, Samuel S, Zou KH, Loughlin KR. Unenhanced helical CT of ureteral stones: a replacement for excretory urography in planning treatment. AJR Am J Roentgenol 1998;171 (4):1051–1053.

41. Fielding JR, Fox LA, Heller H, et al. Spiral CT in the evaluation of flank pain: overall accuracy and feature analysis. J Comput Assist Tomogr 1997;21 (4):635–638.

42. Katz DS, Lane MJ, Sommer FG. Unenhanced helical CT of ureteral stones: incidence of associated urinary tract findings. AJR Am J Roentgenol 1996; 166(6):1319–1322.

43. Hamm M, Wawroschek F, Weckermann D, et al. Unenhanced helical computed tomography in the evaluation of acute flank pain. Eur Urol 2001;39(4): 460–465.

44. Chen MY, Zagoria RJ, Saunders HS, Dyer RB. Trends in the use of unenhanced helical CT for acute urinary colic. AJR Am J Roentgenol 1999;173 (6):1447–1450.

45. Lin WC, Uppot RN, Li CS, Hahn PF, Sahani DV. Value of automated coronal reformations from 64-section multidetector row computerized tomography in the diagnosis of urinary stone disease. J Urol 2007;178(3 pt 1):907–911; discussion 911.

46. Metser U, Ghai S, Ong YY, Lockwood G, Radomski SB. Assessment of urinary tract calculi with 64-MDCT: the axial versus coronal plane. AJR Am J Roentgenol 2009;192(6):1509–1513.

47. Wang LJ, Wong YC, Chuang CK, et al. Predictions of outcomes of renal stones after extracorporeal shock wave lithotripsy from stone characteristics determined by unenhanced helical computed tomography: a multivariate analysis. Eur Radiol 2005;15 (11):2238–2243.

48. Yoshida S, Hayashi T, Morozumi M, Osada H, Honda N, Yamada T. Three-dimensional assessment of urinary stone on non-contrast helical computed tomography as the predictor of stonestreet formation after extracorporeal shock wave lithotripsy for stones smaller than 20 mm. Int J Urol 2007;14(7): 665–667.

49. Dretler SP, Spencer BA. CT and stone fragility. J Endourol 2001;15(1):31–36.

50. Bellin MF, Renard-Penna R, Conort P, et al. Helical CT evaluation of the chemical composition of urinary tract calculi with a discriminant analysis of CT-attenuation values and density. Eur Radiol 2004;14(11):2134–2140.

51. Kim SC, Burns EK, Lingeman JE, Paterson RF, McAteer JA, Williams JC Jr. Cystine calculi: correlation of CT-visible structure, CT number, and stone morphology with fragmentation by shock wave lithotripsy. Urol Res 2007;35(6):319–324.

52. Mostafavi MR, Ernst RD, Saltzman B. Accurate determination of chemical composition of urinary calculi by spiral computerized tomography. J Urol 1998;159(3):673–675.

53. Motley G, Dalrymple N, Keesling C, Fischer J, Harmon W. Hounsfield unit density in the determination of urinary stone composition. Urology 2001;58(2):170–173.

54. Matlaga BR, Kawamoto S, Fishman E. Dual source computed tomography: a novel technique to determine stone composition. Urology 2008;72 (5):1164–1168.

55. Dalla Palma L, Pozzi-Mucelli R, Stacul F. Present-day imaging of patients with renal colic. Eur Radiol 2001;11(1):4–17.

56. Ketelslegers E, Van Beers BE. Urinary calculi: improved detection and characterization with thin-slice multidetector CT. Eur Radiol 2006;16(1): 161–165.

57. Memarsadeghi M, Heinz-Peer G, Helbich TH, et al. Unenhanced multidetector row CT in patients suspected of having urinary stone disease: effect of section width on diagnosis. Radiology 2005;235(2):530–536.

58. Park S, Pearle MS. Imaging for percutaneous renal access and management of renal calculi. Urol Clin North Am 2006;33(3):353–364.

59. Spencer BA, Wood BJ, Dretler SP. Helical CT and ureteral colic. Urol Clin North Am 2000;27(2): 231–241.

60. Eisner BH, Shaikh M, Uppot RN, Sahani DV, Dretler SP. Genitourinary imaging with noncontrast computerized tomography: are we missing duplex ureters? J Urol 2008;179(4):1445–1448.

61. Bruce RG, Munch LC, Hoven AD, et al. Urolithiasis associated with the protease inhibitor indinavir. Urology 1997;50(4):513–518.

62. Blake SP, McNicholas MM, Raptopoulos V. Nonopaque crystal deposition causing ureteric obstruction in patients with HIV undergoing indinavir therapy. AJR Am J Roentgenol 1998;171(3):717–720.

63. Kawashima A, Sandler CM, Boridy IC, Takahashi N, Benson GS, Goldman SM. Unenhanced helical CT of ureterolithiasis: value of the tissue rim sign. AJR Am J Roentgenol 1997;168(4):997–1000.

64. Tanrikut C, Sahani D, Dretler SP. Distinguishing stent from stone: use of bone windows. Urology 2004;63(5):823–826; discussion 826–827.

65. Coll DM, Varanelli MJ, Smith RC. Relationship of spontaneous passage of ureteral calculi to stone size and location as revealed by unenhanced helical CT. AJR Am J Roentgenol 2002;178(1):101–103.

66. Eisner BH, Kambadakone A, Monga M, et al. Computerized tomography magnified bone windows are superior to standard soft tissue windows for accurate measurement of stone size: an in vitro and clinical study. J Urol 2009;181(4):1710–1715.

67. Williams JC Jr, Paterson RF, Kopecky KK, Lingeman JE, McAteer JA. High resolution detection of internal structure of renal calculi by helical computerized tomography. J Urol 2002;167(1): 322–326.

68. Zarse CA, Hameed TA, Jackson ME, et al. CT visible internal stone structure, but not Hounsfield unit value, of calcium oxalate monohydrate (COM) calculi predicts lithotripsy fragility in vitro. Urol Res 2007;35(4):201–206.

69. Ngo TC, Assimos DG. Uric acid nephrolithiasis: recent progress and future directions. Rev Urol 2007;9(1):17–27.

70. Perks AE, Schuler TD, Lee J, et al. Stone attenuation and skin-to-stone distance on computed tomography predicts for stone fragmentation by shock wave lithotripsy. Urology 2008;72(4):765–769.

71. Sheir KZ, Mansour O, Madbouly K, Elsobky E, Abdel-Khalek M. Determination of the chemical composition of urinary calculi by noncontrast spiral computerized tomography. Urol Res 2005;33 (2):99–104.

72. Dretler SP. Calculus breakability: fragility and durility. J Endourol 1994;8(1):1–3.

73. Rassweiler JJ, Renner C, Chaussy C, Thüroff S. Treatment of renal stones by extracorporeal shock-wave lithotripsy: an update. Eur Urol 2001;39(2): 187–199.

74. Renner C, Rassweiler J. Treatment of renal stones by extracorporeal shock wave lithotripsy. Nephron 1999;81(suppl 1):71–81.

75. Deveci S, Coşkun M, Tekin MI, Peşkircioglu L, Tarhan NC, Ozkardeş H. Spiral computed tomography: role in determination of chemical compositions of pure and mixed urinary stones—an in vitro study. Urology 2004;64(2):237–240.

76. Ramakumar S, Patterson DE, LeRoy AJ, et al. Prediction of stone composition from plain radiographs: a prospective study. J Endourol 1999;13 (6):397–401.

77. da Silva SF, Silva SL, Daher EF, Silva Junior GB, Mota RM, Bruno da Silva CA. Determination of urinary stone composition based on stone morphology: a prospective study of 325 consecutive patients in an emerging country. Clin Chem Lab Med 2009;47(5):561–564.

78. Fletcher JG, Takahashi N, Hartman R, et al. Dual-energy and dual-source CT: is there a role in the abdomen and pelvis? Radiol Clin North Am 2009;47(1):41–57.

79. Flohr TG, McCollough CH, Bruder H, et al. First performance evaluation of a dual-source CT (DSCT) system. Eur Radiol 2006;16(2):256–268.

80. Johnson TR, Krauss B, Sedlmair M, et al. Material differentiation by dual energy CT: initial experience. Eur Radiol 2007;17(6):1510–1517.

81. Graser A, Johnson TR, Bader M, et al. Dual energy CT characterization of urinary calculi: initial in vitro and clinical experience. Invest Radiol 2008;43(2):112–119.

82. Primak AN, Fletcher JG, Vrtiska TJ, et al. Noninvasive differentiation of uric acid versus non-uric acid kidney stones using dual-energy CT. Acad Radiol 2007;14(12):1441–1447.

83. Stolzmann P, Kozomara M, Chuck N, et al. In vivo identification of uric acid stones with dual-energy CT: diagnostic performance evaluation in patients. Abdom Imaging 2009 Sep 2. [Epub ahead of print]

84. Bilen CY, Koçak B, Kitirci G, Danaci M, Sarikaya S. Simple trigonometry on computed tomography helps in planning renal access. Urology 2007;70 (2):242–245; discussion 245.

85. El-Nahas AR, El-Assmy AM, Mansour O, Sheir KZ. A prospective multivariate analysis of factors predicting stone disintegration by extracorporeal shock wave lithotripsy: the value of high-resolution noncontrast computed tomography. Eur Urol 2007; 51(6):1688–1693; discussion 1693–1694.

86. Jacobs BL, Smaldone MC, Smaldone AM, Ricchiuti DJ, Averch TD. Effect of skin-to-stone distance on shockwave lithotripsy success. J Endourol 2008; 22(8):1623–1627.

87. Küpeli B, Gürocak S, Tunç L, Senocak C, Karaoğlan U, Bozkirli I. Value of ultrasonography and helical computed tomography in the diagnosis of stone-free patients after extracorporeal shock wave lithotripsy (USG and helical CT after SWL). Int Urol Nephrol 2005;37(2):225–230.

88. Beck EM, Riehle RA Jr. The fate of residual fragments after extracorporeal shock wave lithotripsy monotherapy of infection stones. J Urol 1991;145 (1):6–9; discussion 9–10.

89. Delvecchio FC, Preminger GM. Management of residual stones. Urol Clin North Am 2000;27(2): 347–354.

90. Nakamoto T, Sagami K, Yamasaki A, et al. Long-term results of endourologic treatment of urinary calculi: investigation of risk factors for recurrence or regrowth. J Endourol 1993;7(4):297–301.

91. Zanetti GR, Montanari E, Guarneri A, Trinchieri A, Mandressi A, Ceresoli A. Long-term followup after extracorporeal shock wave lithotripsy treatment of kidney stones in solitary kidneys. J Urol 1992;148(3 pt 2):1011–1014.

92. Pearle MS, Watamull LM, Mullican MA. Sensitivity of noncontrast helical computerized tomography and plain film radiography compared to flexible nephroscopy for detecting residual fragments after percutaneous nephrostolithotomy. J Urol 1999;162 (1):23–26.

93. Waldmann TB, Lashley DB, Fuchs EF. Unenhanced computerized axial tomography to detect retained calculi after percutaneous ultrasonic lithotripsy. J Urol 1999;162(2):312–314.

94. Osman Y, El-Tabey N, Refai H, et al. Detection of residual stones after percutaneous nephrolithotomy: role of nonenhanced spiral computerized tomography. J Urol 2008;179(1):198–200; discussion 200.

95. Katz DS, Venkataramanan N, Napel S, Sommer FG. Can low-dose unenhanced multidetector CT be used for routine evaluation of suspected renal colic? AJR Am J Roentgenol 2003;180(2):313–315.

96. Spielmann AL, Heneghan JP, Lee LJ, Yoshizumi T, Nelson RC. Decreasing the radiation dose for renal stone CT: a feasibility study of single- and multidetector CT. AJR Am J Roentgenol 2002; 178(5):1058–1062.

97. Brenner DJ, Hall EJ. Computed tomography: an increasing source of radiation exposure. N Engl J Med 2007;357(22):2277–2284.

98. Tack D, Sourtzis S, Delpierre I, de Maertelaer V, Gevenois PA. Low-dose unenhanced multidetector CT of patients with suspected renal colic. AJR Am J Roentgenol 2003;180(2):305–311.

99. Ciaschini MW, Remer EM, Baker ME, Lieber M, Herts BR. Urinary calculi: radiation dose reduction of 50% and 75% at CT—effect on sensitivity. Radiology 2009;251(1):105–111.

100. Denton ER, Mackenzie A, Greenwell T, Popert R, Rankin SC. Unenhanced helical CT for renal colic: is the radiation dose justifiable? Clin Radiol 1999; 54(7):444–447.

101. Meagher T, Sukumar VP, Collingwood J, et al. Low dose computed tomography in suspected acute renal colic. Clin Radiol 2001;56(11):873–876.

102. Wall BF, Hart D. National Radiological Protection Board: revised radiation doses for typical X-ray examinations—report on a recent review of doses to patients from medical X-ray examinations in the UK by NRPB. Br J Radiol 1997;70(833):437–439.

103. Mulkens TH, Daineffe S, De Wijngaert R, et al. Urinary stone disease: comparison of standard-dose and low-dose with 4D MDCT tube current modulation. AJR Am J Roentgenol 2007;188(2): 553–562.

104. Hamm M, Knopfle E, Wartenberg S, Wawroschek F, Weckermann D, Harzmann R. Low dose unenhanced helical computerized tomography for the evaluation of acute flank pain. J Urol 2002;167(4): 1687–1691.

105. Kalra MK, Maher MM, Toth TL, et al. Techniques and applications of automatic tube current modulation for CT. Radiology 2004;233(3):649–657.

106. Lee CH, Goo JM, Ye HJ, et al. Radiation dose modulation techniques in the multidetector CT era: from basics to practice. RadioGraphics 2008; 28(5):1451–1459.

107. Kalra MK, Maher MM, Toth TL, Kamath RS, Halpern EF, Saini S. Radiation from "extra" images acquired with abdominal and/or pelvic CT: effect of automatic tube current modulation. Radiology 2004;232(2):409–414.

108. Kim BS, Hwang IK, Choi YW, et al. Low-dose and standard-dose unenhanced helical computed tomography for the assessment of acute renal colic: prospective comparative study. Acta Radiol 2005; 46(7):756–763.

109. Nakayama Y, Awai K, Funama Y, et al. Abdominal CT with low tube voltage: preliminary observations about radiation dose, contrast enhancement, image quality, and noise. Radiology 2005;237(3): 945–951.

110. Funama Y, Awai K, Nakayama Y, et al. Radiation dose reduction without degradation of low-contrast detectability at abdominal multisection CT with a low tube voltage technique: phantom study. Radiology 2005;237(3):905–910.

RadioGraphics

# New and Evolving Concepts in the Imaging and Management of Urolithiasis: Urologists' Perspective

*Avinash R. Kambadakone, MD, FRCR • Brian H. Eisner, MD • Onofrio Antonio Catalano, MD • Dushyant V. Sahani, MD*

**Page 606**

The most important factors influencing decisions regarding urologic intervention are stone location, size, and composition, and patient symptoms (Figs 2, 3) (22).

**Page 608**

CT has several advantages over other imaging techniques: It can be performed rapidly, does not require the administration of contrast material, is highly sensitive for the detection of stones of all sizes, and allows the detection of other unsuspected extraurinary and urinary abnormalities (12,36,38).

**Page 611**

Ege et al (37) reported that stones greater than 6 mm in diameter in the proximal ureter accompanied by more than five secondary signs of obstruction are more likely to necessitate intervention such as endoscopic removal or lithotripsy than are those with fewer secondary signs.

**Page 614**

Determination of stone composition is of particular importance because *(a)* uric acid stones may be treated with urinary alkalinization as a first-line treatment, with surgical treatment being reserved for stones that do not respond to medical therapy; and *(b)* stones of certain compositions (eg, cystine stones), as well as calcium-based stones of certain attenuation, are extremely difficult to fragment with SWL (51,69–71).

**Page 616**

The purpose of imaging following either urologic intervention or medical therapy is essentially threefold: to confirm stone-free status, to identify the presence of residual stones, and to rule out obstruction in the urinary system (58).